A faster precession parameter to interpret gravitational-wave data

Diego Fernando Padilla Monroy[1], Davide Gerosa[2]
[1] *Florida International University*
[2] *Universitá degli Studi di Milano-Bicocca*
(University of Florida IREU program)
(Dated: Summer 2022)

The effective precession parameter χ_p is a widely used quantity to study precession of the orbital plane in binary black-hole merger events analyzed studying their gravitational-wave emission by LIGO and VIRGO groups. Nevertheless, the current definition of χ_p does not characterize the precession dynamics properly for all binary black-hole systems and a generalization of the previous χ_p was proposed. In this report we explore yet another generalization of the precession parameter and compare it with the other χ_p formulations and find (i) no significant difference between the posterior distributions of the ***generalized*** χ_ps for all current gravitational-wave events and (2) a $\approx 10^4$ factor improvement in the computation time with the new generalization proposed in this report, compared with the other proposed generalization .

I. INTRODUCTION

Precession of the orbital plane in binary black-hole merger events has an important role modulating the gravitational-wave emitted by these systems [1]. It has thus been key for the rising field of gravitational-waves to understand this phenomenon deeply and use it to produce accurate waveform models.

In addition to this, previous studies have shown that the formation channel of a binary black-hole has an impact on the spin misalignment of the black-holes with respect to the orbital angular momentum of the system [2]. Furthermore, as noted in [1], this spin misalignment gives rise to orbital plane precession in the binary system. It is clear that acquiring a deep understanding of this phenomenon has important astrophysical implications.

To capture this information from gravitational-wave detections, the precession parameter $\chi_p^{heuristic}$ was first introduced by [3]. In current data analysis it is considered that a confident measurement of $\chi_p^{heuristic}$ away from zero with significant information gain from the prior is a strong indication of orbital plane precession [4]. Nevertheless, $\chi_p^{heuristic}$ was shown to only capture the plane precession dynamics for binary black-hole systems in which one of the spins dominates the precession (The dominating black-hole is more massive and has higher spin magnitude). In order to generalize $\chi_p^{heuristic}$ to all possible binary black-hole systems Davide et. al. [4] proposed $\chi_p^{averaged}$. Although this new precession parameter was shown to correctly capture the orbital plane precession, its computation time is considerably high due to a non-analytical integral in its formulation. Because of this, in this report we explore a new generalization of $\chi_p^{heuristic}$ which is analytical and compare it with the previous generalization.

II. QUANTIFYING PRECESSION

A. Defining the precession parameters

Let us define the quantities needed to describe a binary black-hole merger system. $M = m_1 + m_2$ (Total mass of the system with black-holes with masses $m_2 \leq m_1$), $q = m_2/m_1$ (Mass ratio), $\mathbf{S_{1,2}}$ (Spins of the black-holes), $\chi_{1,2}$ (Dimensionless spin magnitudes) and r is the orbital separation between the black-holes. We employ geometric units $G = c = 1$.

We also study or system in terms of the following:

$$\cos\theta_1 = \hat{\mathbf{S}}_1 \cdot \hat{\mathbf{L}} \tag{1}$$

$$\cos\theta_2 = \hat{\mathbf{S}}_2 \cdot \hat{\mathbf{L}} \tag{2}$$

$$\cos\Delta\Phi = \frac{\hat{\mathbf{S}}_1 \times \hat{\mathbf{L}}}{|\hat{\mathbf{S}}_1 \times \hat{\mathbf{L}}|} \cdot \frac{\hat{\mathbf{S}}_2 \times \hat{\mathbf{L}}}{|\hat{\mathbf{S}}_2 \times \hat{\mathbf{L}}|} \tag{3}$$

Where $\hat{\mathbf{L}}$ is the direction of the orbital angular momentum of the system.

From equation (10) in [4], the orbit-averaged evolution of the direction of the orbital angular momentum unit vector, that is, the precession of the orbital plane, has this form:

$$\left|\frac{d\hat{\mathbf{L}}}{dt}\right|^2 = (\Omega_1\chi_1\sin\theta_1)^2 + (\Omega_2\chi_2\sin\theta_2)^2 + 2\Omega_1\Omega_2\chi_1\chi_2\sin\theta_1\sin\theta_2\cos\Delta\Phi \tag{4}$$

Here, Ω_1 and Ω_2 are defined as follows in [4]:

$$\Omega_1 = \frac{M^2}{2r^3(1+q)^2}[4 + 3q - \frac{3q\chi_{eff}}{1+q}\frac{M^2}{L}] + \mathcal{O}(\frac{M^4}{L^2}) \tag{5}$$

$$\Omega_2 = \frac{qM^2}{2r^3(1+q)^2}[4q + 3 - \frac{3q\chi_{eff}}{1+q}\frac{M^2}{L}] + \mathcal{O}(\frac{M^4}{L^2}) \tag{6}$$

Where:

$$\chi_{eff} = \frac{\chi_1\cos\theta_1 + \chi_2\cos\theta_2}{1+q} \tag{7}$$

From these quantities, [3] defined χ_p as follows:

$$\chi_p^{heuristic} = \max(\chi_1 \sin\theta_1, \frac{\Omega_2}{\Omega_1}\chi_2 \sin\theta_2) \tag{8}$$

Nevertheless, Davide et. al. [4] showed that this definition does not work for all binary black-hole systems, because it doesn't take into account $\Delta\Phi$, which is a quantity that changes in the same timescale (precession timescale) as θ_1 and θ_2.

To find a better precession parameter, [4] averaged over the square root of (4) (normalized by $\frac{1}{\Omega_1}$) using the following expression:

$$\chi_p^{averaged} = \frac{\int \left|\frac{d\hat{\mathbf{L}}}{dt}\right| \frac{1}{\Omega_1}(\frac{d\psi}{dt})^{-1} d\psi}{\int (\frac{d\psi}{dt})^{-1} d\psi} \tag{9}$$

Here, $\psi(t)$ is a function that parameterizes the precession dynamics. For the current analysis, we choose $\psi = |\mathbf{S_1} + \mathbf{S_2}|$, the magnitude of the total spin of the system.

In order to do the averaging, the three quantities that describe the system; θ_1, θ_2 and $\Delta\Phi$ have to be expressed as functions of S. Those equations are in appendix of [4]:

$$\cos\theta_1(S) = \frac{1}{2(1-q)S_1}\left[\frac{J^2 - L^2 - S^2}{L} - \frac{2qM^2\chi_{eff}}{1+q}\right], \tag{10}$$

$$\cos\theta_2(S) = \frac{q}{2(1-q)S_1}\left[-\frac{J^2 - L^2 - S^2}{L} + \frac{2qM^2\chi_{eff}}{1+q}\right], \tag{11}$$

$$\cos\Delta\Phi(S) = \frac{S^2 - S_1^2 - S_2^2 - 2S_1S_2\cos\theta_1(S)\cos\theta_2(S)}{2S_1S_2\sin\theta_1(S)\sin\theta_2(S)}, \tag{12}$$

where $J = |S + L|$ is the magnitude of the total angular momentum of the system. Then, the $\left|\frac{dS}{dt}\right|$ term was also found in such appendix and it was obtained from precession equations (Same case as (21) in [5]) and is of this form:

$$\left|\frac{dS}{dt}\right| = \frac{3S_1S_2M^9q^5(1-q)}{2L^5(1+q)^{11}}\left[1 - \frac{qM^2\chi_{eff}}{(1+q)^2L}\right] \times \frac{\sin\theta_1(S)\sin\theta_2(S)\left|\sin\Delta\Phi(S)\right|}{S}. \tag{13}$$

The $\left|\frac{d\hat{\mathbf{L}}}{dt}\right|$ term is readily obtained by plugging in equations (10-12) in (4).

The final pieces are the integration limits (maximum and minimum allowed total spin magnitudes). Other studies have obtained this quantities in different ways. In [6] two "effective potentials" were defined such that they enclose all allowed values of $S = |\mathbf{S_1} + \mathbf{S_2}|$. In [5], using orbit averaged equations for the evolution of $\hat{\mathbf{S}}_1$, $\hat{\mathbf{S}}_2$ and $\hat{\mathbf{L}}$, the evolution equation of S^2 was derived (Analogous equation to (13)). After simpifications, the two approaches arrive to a cubic polynomial in S^2 (Equation 21 in [5] and equation 16a in [6] which has three real roots, $S_3^2 < S_-^2 < S_+^2$; S_-^2 is the minimum allowed total spin magnitude and S_+^2 the maximum. The same result can be replicated using equation (13).

When applying the (9) with the previous described quantities, the numerator becomes this integral

$$\int_{S_-}^{S_+} 2S\sqrt{\frac{n_2S^4 + n_1S^2 + n_0}{-(S^2 - S_+^2)(S^2 - S_-^2)(S^2 - S_3^2)}}dS. \tag{14}$$

The coefficients of the polynomial in the numerator of the square root can be easily obtained from (4) and (10-12). It is remarkable that this integral can only be solved numerically. That heavily impacts computation time for each $\chi_p^{averaged}$ (The denominator of (9), in contrast, can be solved analytically). Given that, in average, the amount of data points in the posterior samples of all gravitational-wave data release is $\approx$ 70000, using this $\chi_p^{averaged}$ could be too costly in computation time for research groups without access to clusters. We thus explore the slightly modified formulation:

$$\chi_p^{RMS} = \sqrt{\frac{\int \left|\frac{d\hat{\mathbf{L}}}{dt}\right|^2 \frac{1}{\Omega_1}(\frac{d\psi}{dt})^{-1} d\psi}{\int (\frac{d\psi}{dt})^{-1} d\psi}}. \tag{15}$$

To get a first glance of how this new formulation compares with $\chi_p^{averaged}$, we use Jensen's inequality [7] and know that $< x^2 > \; > \; < x >^2$ when x is not a constant. Taking the square root in both sides, $\sqrt{< x^2 >} \; > \; < x >$. This tells us that χ_p^{RMS} is always going to be greater than $\chi_p^{averaged}$.

Employing χ_p^{RMS}, all the integrals involved in the computation can be solved in terms of complete elliptic integrals of the first and second kind ($K(m)$ and $E(m)$) respectively. To simplify the notation, allow us to define:

$$\rho = \sqrt{S_+^2 - S_3^2} \tag{16}$$

$$\lambda = \frac{S_+^2 - S_-^2}{\rho^2} \tag{17}$$

These are those integrals and their solutions:

$$\int_{S_-^2}^{S_+^2} \frac{n_0}{\sqrt{-(S^2 - S_+^2)(S^2 - S_-^2)(S^2 - S_3^2)}}dS^2 = \frac{2n_o}{\rho}K(\lambda) \tag{18}$$

$$\int_{S_-^2}^{S_+^2} \frac{S^2 n_1}{\sqrt{-(S^2-S_+^2)(S^2-S_-^2)(S^2-S_3^2)}} dS^2 = \frac{2S_3^2 n_1}{\rho} K(\lambda) + 2n_1 \rho E(\lambda) \tag{19}$$

$$\int_{S_-^2}^{S_+^2} \frac{S^4 n_2}{\sqrt{-(S^2-S_+^2)(S^2-S_-^2)(S^2-S_3^2)}} dS^2 = \frac{2n_2}{3\rho}(2\rho^2(S_+^2+S_-^2+S_3^2)E(\lambda) + (S_+^2(S_3^2-S_-^2)+S_3^2(S_-^2+2S_3^2))K(\lambda)). \tag{20}$$

B. Relation between χ_p^{RMS} and $\chi_p^{heuristic}$

We do a parallel exercise as the one done in [4] in which we study equation (15) in the limit that spin-spin couplings can be neglected compared to spin-orbit couplings. We do this because in that limit the precession dynamics are dominated by just one of the spins and that is the type of system for which $\chi_p^{heuristic}$ was intended to capture the precession dynamics.

In this set-up of binary black-hole merger, $\mathbf{S_1}$ and $\mathbf{S_2}$ precess with constant velocity and inclination angles over $\mathbf{L}$. These conditions imply: $\frac{d\theta_1}{dt} = \frac{d\theta_2}{dt} = \frac{d^2\Delta\Phi}{dt^2} = 0$. Under this conditions, we can set $\psi(t) = \Delta\Phi$, because that quantity can characterize the precession dynamics on its own. Then equation (15) becomes:

$$\chi_p^{RMS} = \sqrt{\frac{1}{2\pi}\int_0^{2\pi} \chi_p^2 d\Delta\Phi} = \sqrt{(\chi_1 \sin(\theta_1))^2 + (\chi_2 \tilde{\Omega} \sin(\theta_2))^2} \tag{21}$$

For shorter notation, let's use:

$$Max = \max(\chi_1 \sin\theta_1, \frac{\Omega_2}{\Omega_1}\chi_2 \sin\theta_2) \tag{22}$$

$$Min = \min(\chi_1 \sin\theta_1, \frac{\Omega_2}{\Omega_1}\chi_2 \sin\theta_2) \tag{23}$$

$$\delta\chi = Max/Min \tag{24}$$

We can rewrite χ_p^{RMS} in terms of Max and Min:

$$\chi_p^{RMS} = \sqrt{Max^2 + Min^2} \tag{25}$$

Finally we perform a Maclaurin series on Min and find:

$$\chi_p^{RMS} = Max(1 + \frac{\delta\chi^2}{2} + \mathcal{O}(\delta\chi^4)), \tag{26}$$

which is very similar to equation (21) on [4] and confirms that χ_p^{RMS}, to first order in Min, reduces to $\chi_p^{heuristic}$. This means that when the precession dynamics is heavily dominated by one of the spins, the two definitions of χ_p are fairly similar, which is exactly what we expect from χ_p^{RMS} if we claim that it generalizes $\chi_p^{heuristic}$. For comparison, the exact same calculation for $\chi_p^{averaged}$ yields [4]:

$$\chi_p^{averaged} = Max(1 + \frac{\delta\chi^2}{4} + \mathcal{O}(\delta\chi^4)) \tag{27}$$

III. COMPARING PRECESSION PARAMETERS

A. Testing in simulated data

In order to contrast how the different precession parameter formulations behave in different scenarios ($q, \chi_1 and \chi_2$), with the aid of the code [8], orbit averaged simulations of binary black-hole mergers were performed. The results are encapsulated in Figure 1. It is clear that the new precession parameter χ_p^{RMS} correctly captures $\left|\frac{d\hat{\mathbf{L}}}{dt}\right|$ while also smoothing out the precession timescale variations for all scenarios, both when the precession is dominated by only one spin (bottom two panels) and when there is a big contribution from both spins (top two panels). The agreement between χ_p^{RMS} and $\chi_p^{Averaged}$ is also remarkable, as it seems that in all mergers studied the difference is minimal if compared with the difference between $\chi_p^{Averaged}$ and $\chi_p^{heuristic}$. We see no difference between the numerical and analytical implementations of χ_p^{RMS}, which tells us that equations (18-20) are correct. Also, we note that χ_p^{RMS} is always bigger than $\chi_p^{averaged}$ as expected. Finally, careful inspection of the red and black (with yellow dashes) curves, reveal some small fluctuations. This is because of the breaking down of the timescale hierarchy in binary black holes [4].

Further exploring the different formulations, we computed 2500 precession parameters of binary black-hole mergers with isotropically distributed spins (here we chose $\hat{\mathbf{L}} = \hat{\mathbf{z}}$) and for different q, χ_1 and χ_2 to see the statistical behavior of the different definitions of χ_p. The resulting distributions are displayed in Figure 2. We notice that, as expected, χ_p^{RMS} is not bounded by 1 (unlike $\chi_p^{heuristic}$) but by 2; the same as $\chi_p^{averaged}$.

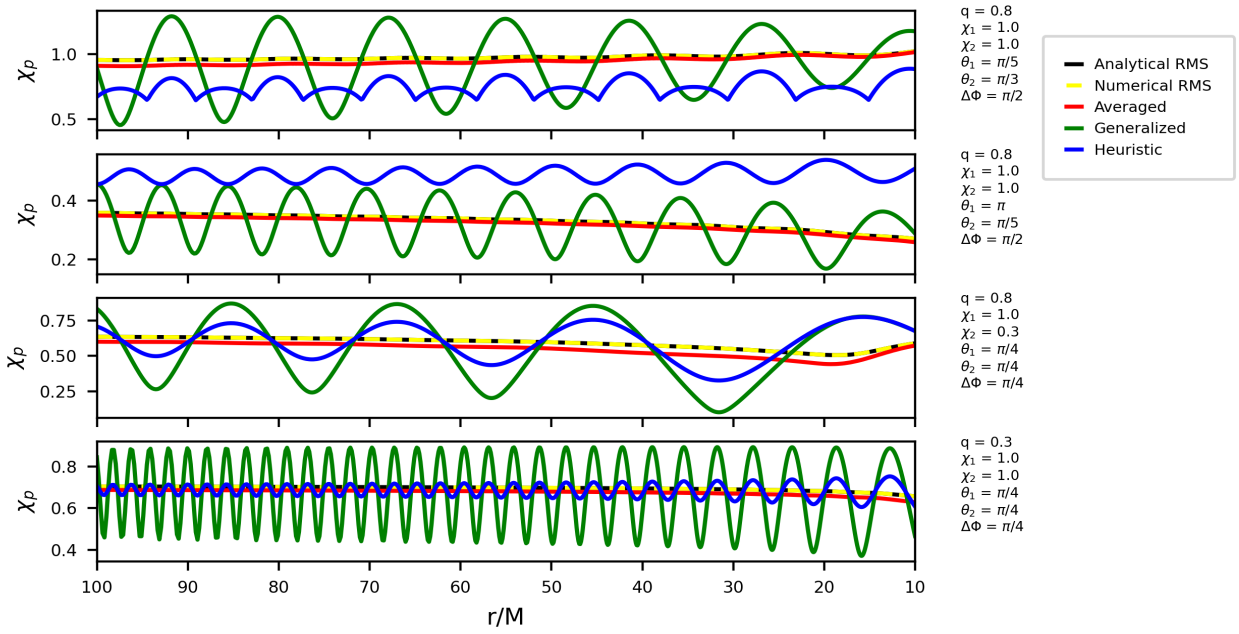

Figure 1. Evolution of χ_p in the during the inspiral of 4 different binary black-hole systems. The green line corresponds to $\left|\frac{d\mathbf{L}}{dt}\right| \frac{1}{\Omega_1}$, that is, the most general expression for the precession parameter which maintains all the precession timescale variations; $\chi_p^{averaged}$ (red line) and χ_p^{RMS} (black line) are intended to smooth out those variations. We also display $\chi_p^{heuristic}$ (blue line) and the dashed yellow line also represents χ_p^{RMS}, but computed numerically instead of with equations (18-20).

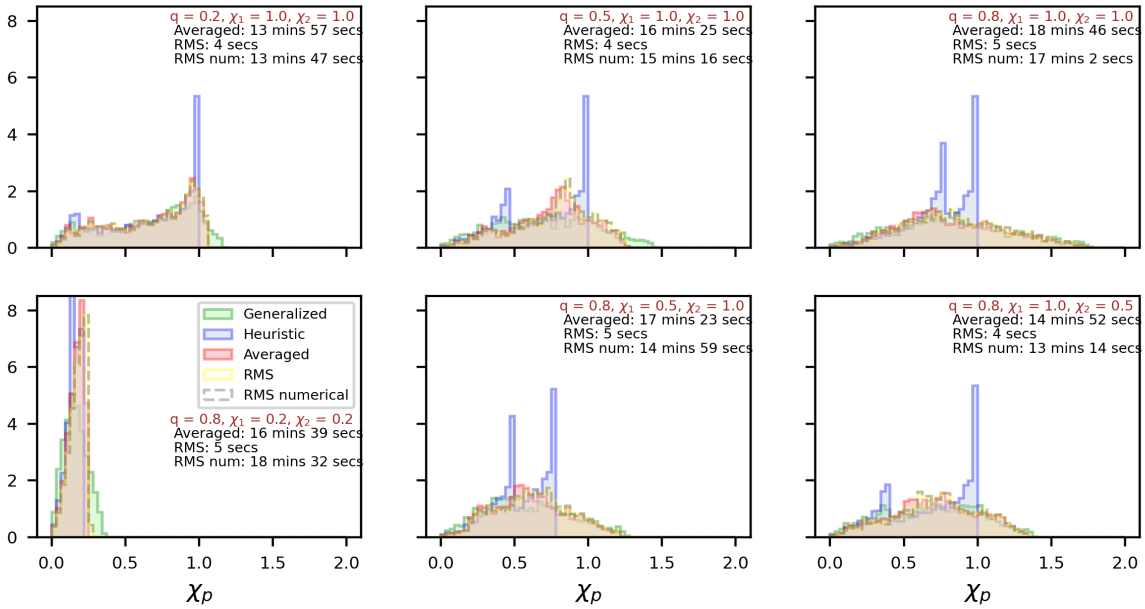

Figure 2. Distribution of different χ_p formulations for 2500 binary black-hole mergers with isotropically distributed spins. Each panel includes parameters computed with different q, χ_1 and χ_2 values. The computation time of χ_p^{RMS} (analytical and numerical) and $\chi_p^{heuristic}$ are also displayed.

As explained in [4], the generalized definitions of χ_p go over 1 when there is strong influence of the two spins causing the orbital plane precession. In the plots in Figure two we also recorded the time it took to produce the histograms. From these numbers, we can do a first comparison on computation times (Processor used: Intel(R) Core(TM) i5-9300H CPU @ 2.40 GHz). We find a ≈ 190 factor improvement in computation time using $\chi_p^{heuristic}$ instead of $\chi_p^{averaged}$ and a ≈ 185 factor improvement when comparing the analytical and numerical implementation of our new proposed precession parameter. These are significant improvements, but in order to directly test its applicability to state of the art gravitational-wave analysis, we shall compare all χ_p formulations for gravitational wave data.

B. Testing in all GW events

As for the analysis done in [4], only few gravitational-wave events showed big discrepancies between $\chi_p^{heuristic}$ and $\chi_p^{averaged}$. Nevertheless, that study was only done with less GW from the LIGO/Virgo detectors. In this report we plot the different χ_p posterior distributions for all gravitational-waves on O1, O2.1 and O3 catalogs.

For the O1 catalog, we used the publicly released samples from [9], which use the IMRPhenomPv2 waveform. For catalog O2.1 we used the IMRPhenomXPHM waveform model except for GW190425_081805, for which we used IMRPhenomPv2_NRTidal:HighSpin. Finally, for catalog O3 we also used the IMRPhenomXPHM waveform for all gravitational-waves, except for GW200115_042309, GW200105_162426 and GW191219_163120 for which an equal mix of the waveforms IMRPhenomXPHM and SEOBNRv4PHM are used [10]. The results are displayed in Figure 3 and Figure 4. We found that for most events, χ_p^{RMS} and $\chi_p^{averaged}$ overlap almost perfectly. In order to further check the agreement, we plotted against each other the medians of the posterior distribution of both formulations. Figure 5 (left) displays this. As it is readily observed, the trend we see is that the two formulations yield the same median for all gravitational-wave events recorded so far. This finding shows that the new precession parameter χ_p^{RMS} can in fact be used interchangeably with $\chi_p^{averaged}$. In Figure 5 (left) there is also a comparison between 2 standard deviations of the posteriors of χ_p^{RMS} and $\chi_p^{averaged}$. This plot gives us information about the spread of the posterior, and thus of its uncertainty. We see that, just like the with median, the two formulations yield identical results.

Apart from the consistency between both formulations, the most important finding of this study is the improvement of the computation time. We timed the computation time for each of the posteriors and found that, on average (Processor used : Intel(R) Xeon(R) Gold 5220R CPU @ 2.20GHz), using $\chi_p^{averaged}$, the speed found was ~ 5 computations per second, while using χ_p^{RMS} the computation time was $\sim 3.6 \times 10^5$ computations per second. This implies, a 7×10^4 factor improvement in computation time.

There are other pieces of information that can be extracted from the distributions in Figures 3 and 4. As it was pointed out before, this project follows the steps of [4]. Here we expanded Figure 4 in that paper and we found even more events where we see important differences between $\chi_p^{averaged}$ and $\chi_p^{heuristic}$. Some interesting ones which were not studied in the previous study are listed next. GW190728_060333 which is in Fig 3, in Fig 4: GW190805_211137, GW190915_235702 and GW191109_010717. Of course there are other events which also shown disagreement. In fact there are distributions in which not only the generalized χ_ps differ from the heuristic definition, but we also observe that the posteriors of the generalized definitions extend further than one in the x-axis. It would be ideal to check if those events are mergers in which both black-holes could contribute greatly to the precession.

Aiming to complement Figure 5 in [4], we recreate the same plot of medians and spread (2 standard deviations in this case) of $\chi_p^{averaged}$ and $\chi_p^{heuristic}$ posteriors. This is shown in Figure 5 (right). Our findings in this case are that the linear trend shown in Figure 5 of [1] is broken for some more recent gravitational-wave events. In contrast, the comparison of the spread of the posteriors follows the same trend as in [4], showing that $chi_p^{heuristic}$ underestimates the uncertainty. These findings reaffirm the importance of employing the generalized definitions of χ_p (either $\chi_p^{averaged}$ or χ_p^{RMS}). As waveform models and detection sensibility get better, we could find more events with non negligible spin-spin coupling and we should use improved precession estimators as well.

IV. CONCLUSIONS

A new precession parameter formulation has been shown to correctly capture the precession dynamics of all binary black-hole mergers detected by LIGO and Virgo. It was shown in different ways (Equation (25), bottom panels of Figure 1 and several events in Figures 3 and 4), that this new estimator χ_p^{RMS} reduces to $\chi_p^{heuristic}$, the widely used precession estimator, in the limit that one spin-spin couplings can be neglected (very large orbital separations between the black-holes, or one of the black-holes dominates the precession through his mass or spin magnitude). We also saw that χ_p^{RMS} can be interchanged with $\chi_p^{averaged}$ for calculations of the posteriors of all current detected gravitational-waves available (Figure 5 (left)). Furthermore, we found that the definition proposed in this report greatly enhances the computation time compared with $\chi_p^{averaged}$, although we have seen different improvement factors while computing χ_ps.

This might be due to the fact that we used different processors, one for working with simulated data an one

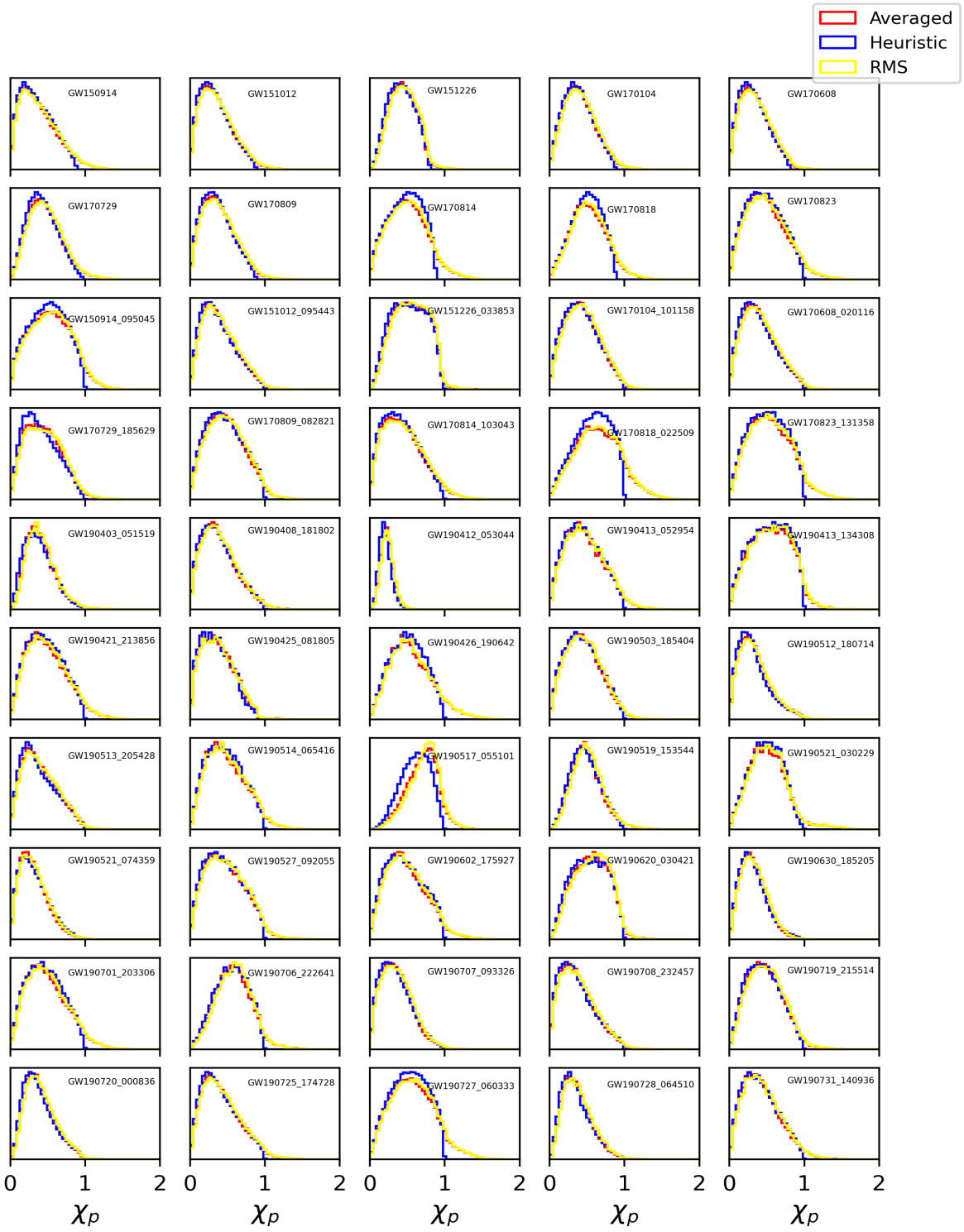

Figure 3. χ_p posterior distributions for O1 and O2.1 catalogs events computed with the three precession parameter formulations discussed in this report. This plot continues Figure 4 in [4], and the allows to explore more gravitational-wave events where $\chi_p^{heuristic}$ is deficient.

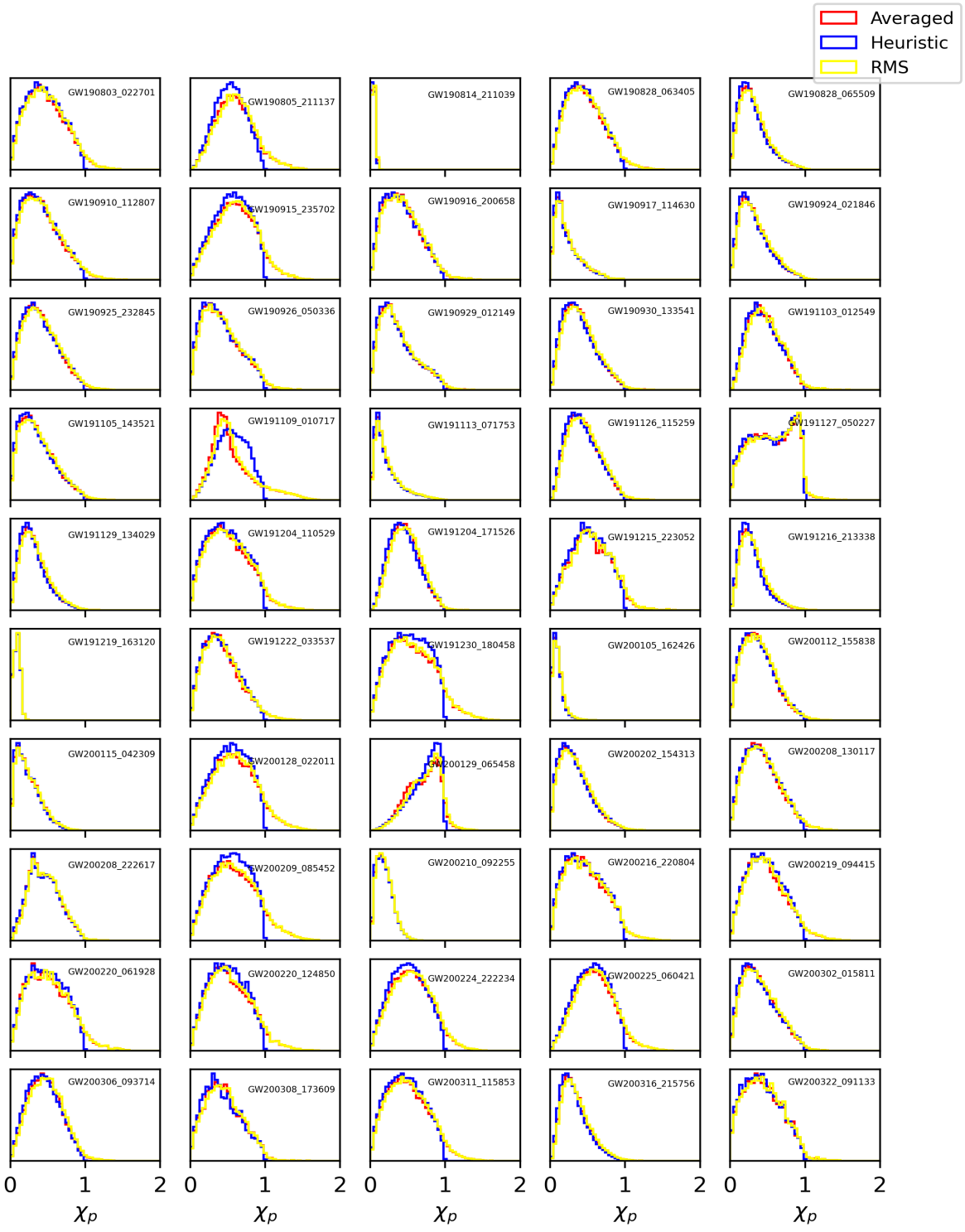

Figure 4. χ_p posterior distributions for O2.1 and O3 catalogs computed with the three precession parameter formulations discussed in this report. All the gravitational waves in this figure are new with respect to Figure 4 in [4].

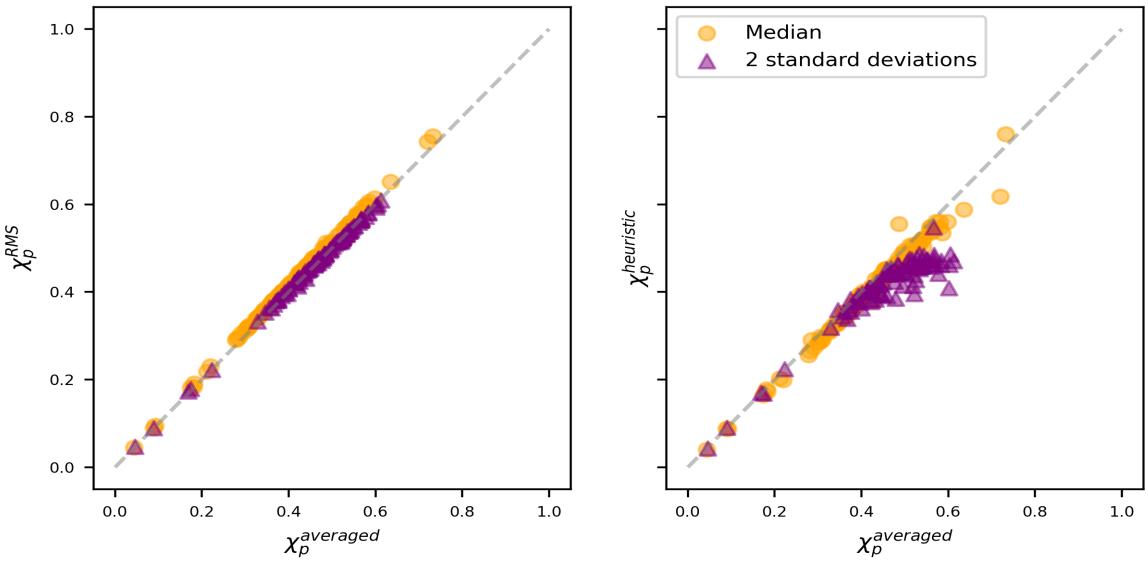

Figure 5. Left Panel: Comparison of medians and two standard deviations of all posteriors shown in Figures 3 and 4 computed with $\chi_p^{averaged}$ and χ_p^{RMS}, the agreement is remarkable. Right Panel: Comparison of medians and two standard deviations of all posteriors shown in Figures 3 and 4 computed with $\chi_p^{averaged}$ and $\chi_p^{heuristic}$, it is remarkable that there is a disagreement in the medians.

for the real LIGO data. For the simulated data, (using Intel(R) Core(TM) i5-9300H CPU @ 2.40 GHz) we found a $\sim$ 190 factor enhancement, for the real gravitational-waves data, (using Intel(R) Xeon(R) Gold 5220R CPU @ 2.20GHz) we found a $\sim 3.6 \times 10^5$ factor improvement. Also, it is important to note that when working with the simulated data we only had 2500 computations to do (See Figure 2), but the average number of computations for Figures 3 and 4 was 70,000. That being said, the speed enhancement is still noticeable in any scenario and we think it would be a useful tool to use, specially for groups without access to clusters.

Other interesting conclusions we get from this study is that with more gravitational-waves been detected, we are finding more binary black-hole mergers in which $\chi_p^{heuristic}$ yields considerably different posterior distributions if compared with the generalized χ_p formulations. As mentioned before, this is yet more interesting since even if some differences like this where also noticeable in Figure 4 in [4] (Comparison of $\chi_p^{heuristic}$ and $\chi_p^{averaged}$ posteriors for less events), the medians of the posteriors seemed to be identical (Figure 5 of that same paper). In contrast with that, this report shows differences in the medians obtained with $\chi_p^{heuristic}$ and $\chi_p^{averaged}$ posteriors; the linear trend from Figure 5 in [4] is broken. This suggests a study in the specific gravitational waves that broke the linearity of the medians.

Finally, we recognize that there are much more studies to be done on these estimators. For example, one could look at the impact of using χ_p^{RMS} in population studies.

V. ACKNOWLEDGMENTS

We thank Dr. Paul Fulda and Dr. Peter Wass from University of Florida for organizing this project. We also thank Daria Gangardt for useful discussions. This project was done through the University of Florida funded by NSF grant number 1460803.

[1] Theocharis A. Apostolatos, Curt Cutler, Gerald J. Sussman, and Kip S. Thorne. Spin-induced orbital precession and its modulation of the gravitational waveforms from merging binaries. *Phys. Rev. D*, 49:6274–6297, Jun 1994.

[2] Thomas A. Callister, Will M. Farr, and Mathieu Renzo. State of the Field: Binary Black Hole Natal Kicks and Prospects for Isolated Field Formation after GWTC-2. *Astrophys. J.*, 920(2):157, 2021.

[3] Patricia Schmidt, Frank Ohme, and Mark Hannam. Towards models of gravitational waveforms from generic binaries: Ii. modelling precession effects with a single effective precession parameter. *Phys. Rev. D*, 91:024043, Jan 2015.

[4] Davide Gerosa, Matthew Mould, Daria Gangardt, Patricia Schmidt, Geraint Pratten, and Lucy M. Thomas. A generalized precession parameter $\chi_{\rm p}$ to interpret gravitational-wave data. *Phys. Rev. D*, 103(6):064067, 2021.

[5] Katerina Chatziioannou, Antoine Klein, Nicolás Yunes, and Neil Cornish. Constructing gravitational waves from generic spin-precessing compact binary inspirals. *Phys. Rev. D*, 95:104004, May 2017.

[6] Davide Gerosa, Michael Kesden, Ulrich Sperhake, Emanuele Berti, and Richard O'Shaughnessy. Multi-timescale analysis of phase transitions in precessing black-hole binaries. *Phys. Rev. D*, 92:064016, 2015.

[7] Jensen inequality encyclopedia of mathematics. `http://encyclopediaofmath.org/index.php?title=Jensen_inequality&oldid=16975`. Accessed: 2022-07-29.

[8] Davide Gerosa and Michael Kesden. PRECESSION: Python toolbox for dynamics of spinning black-hole binaries. Astrophysics Source Code Library, record ascl:1611.004, November 2016.

[9] I. M. Romero-Shaw et al. Bayesian inference for compact binary coalescences with bilby: validation and application to the first LIGO–Virgo gravitational-wave transient catalogue. *Mon. Not. Roy. Astron. Soc.*, 499(3):3295–3319, 2020.

[10] The LIGO Scientific Collaboration, the Virgo Collaboration, the KAGRA Collaboration, R. Abbott, T. D. Abbott, F. Acernese, K. Ackley, C. Adams, N. Adhikari, R. X. Adhikari, and et al. GWTC-3: Compact Binary Coalescences Observed by LIGO and Virgo During the Second Part of the Third Observing Run. *arXiv e-prints*, page arXiv:2111.03606, November 2021.